Journal of Magnetic Resonance **154,** 325–328 (2002)
doi:10.1006/jmre.2001.2497, available online at http://www.idealibrary.com on IDEAL®

COMMUNICATIONS

A New Method for Variable Temperature Gradient Shimming

Clare-Louise Evans,* Gareth A. Morris,*,[1] and Adrian L. Davis†

*Department of Chemistry, University of Manchester, Oxford Road, Manchester M13 9PL, United Kingdom; and †Pfizer Global Research and Development, Sandwich, Kent CT13 9NJ, United Kingdom

Received September 4, 2001; revised November 13, 2001

Sample convection can severely attenuate the signals observed in pulsed field gradient spin–echo experiments such as those used for gradient shimming. A new class of pulse sequences is proposed, in which a double spin–echo refocuses the phase errors caused by sample convection, enabling gradient shimming to be performed reliably over a wide range of temperatures. © 2002 Elsevier Science (USA)

Key Words: **gradient shimming; convection; variable temperature; double spin–echo; homospoil.**

Gradient shimming methods are now used routinely in many laboratories. Typically, these employ proton or deuterium spin or gradient echoes to map the magnetic field within the sample (*1–4*), allowing rapid and efficient convergence to optimum field homogeneity. Such methods are often thought to be incompatible with variable temperature operation, although gradient shimming can often be successful for modest deviations from room temperature. The limiting factor is loss and distortion of the echo signal, for which convection currents arising from temperature gradients within the sample are responsible. A simple modification to existing gradient shimming pulse sequences that provides compensation for the effects of convection is demonstrated. The sequences exhibit good shimming performance throughout the liquid ranges of common solvents.

Pulse sequences for gradient shimming map the spatial distribution of the magnetic field by monitoring the change in signal phase as a function of position when an extra delay is introduced into a spin or gradient echo imaging experiment. Most current applications of gradient shimming are restricted to a single (z) dimension, using a z field gradient to measure profiles of signal as a function of position. Figure 1a shows a simple and widely used one-dimensional (1D) field mapping pulse sequence (*3*) based on the spin echo. Echoes measured for two values of the delay τ differing by an amount $\Delta\tau$ are Fourier transformed to yield signal profiles which are phase shifted as a result of precession during the period $\Delta\tau$. Field maps displaying Larmor frequency as a function of z position (or of frequency within the profile) can be produced by plotting the phase shift divided by $\Delta\tau$ as a function of position. In gradient shimming, a series of such field maps is measured for fixed offsets of different shim currents, allowing the construction of shim maps that describe the field shapes produced by the different shim coils. The corrections necessary to minimize field variation across the sample are then determined by iterative refinement of the shim settings, fitting field maps with the shim maps. Spin echoes are used in preference to gradient echoes as they reduce the signal losses experienced at longer echo times, allowing measurements to benefit from the higher signal-to-noise ratio offered by a low read gradient.

The gradient shimming sequence of Fig. 1a is designed to refocus the signal at the midpoint τ_m of the acquisition time τ_a. The formal requirement for successful refocusing is that the integral of the effective gradient G^* with respect to time be zero:

$$\int_0^{\tau_m} G^*(t)\,dt = 0. \qquad [1]$$

The effective gradient is defined as the actual gradient multiplied by the coherence order. However, where the liquid sample is not stationary, additional phase shifts will arise that are dependent upon the speed and direction of flow (*5, 6*).

The velocity of liquid flow varies with position in a convecting sample, so both the amplitude and the phase of the signal profile measured by an experiment such as Fig. 1a will be affected, reducing its effectiveness in gradient shimming. For an isochromat moving with speed v along a constant gradient G during a simple spin echo 90°–τ–180°–τ, the phase accumulated at time 2τ by virtue of this flow will be

$$\Delta\phi = Gv\tau^2. \qquad [2]$$

For the simple case of a rectangular velocity spectrum, i.e., equal amounts of signal moving at all velocities between $-v_{max}$ and $+v_{max}$, the net signal measured at time 2τ will be proportional to

$$S = \int_{-v_{max}}^{+v_{max}} \exp(iGv\tau^2)\,dv = \frac{2\sin(Gv_{max}\tau^2)}{G\tau^2}. \qquad [3]$$

[1] To whom correspondence should be addressed. Fax: (0) 161 275 4598. E-mail: g.a.morris@man.ac.uk.

1090-7807/02 $35.00

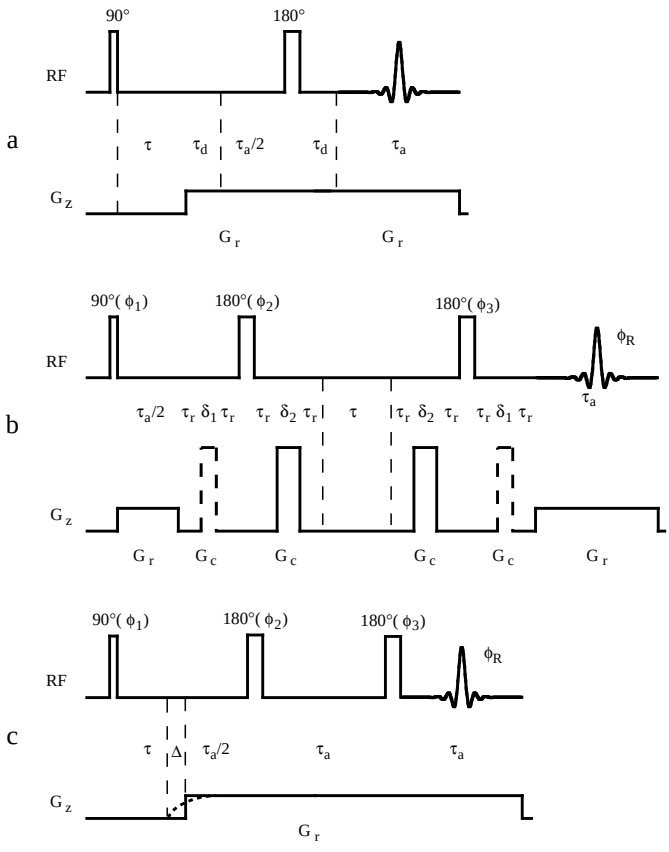

FIG. 1. Pulse sequences for uniaxial gradient shimming. (a) Conventional spin–echo sequence of Ref. (*3*); the extra dephasing time τ_d reduces the need for phase cycling. (b) Flow-compensated double spin–echo sequence using pulsed field gradients. (c) Flow-compensated double spin–echo sequence using homospoil (z shim) field gradient; for the INOVA spectrometer the optimum delay Δ, used to correct for the slow z shim response (dotted line) was 8 ms. Where the optional pulses of width δ_1 are used in sequence (b), the pulse width δ_2 increases according to Eq. [6]. Phase cycling for sequences (b) and (c): $\phi_1 = (x, y, x, y)\,(-x, -y, -x, -y)\,(y, -x, y, -x)\,(-y, x, -y, x)$; $\phi_2 = (x, y)_8$; $\phi_3 = (x, -y, y, x)_4$; $\phi_R = (x, y, -x, -y)\,(-x, -y, x, y)\,(y, -x, -y, x)\,(-y, x, y, -x)$.

Although the actual velocity spectrum in a convecting sample is more complex, the rectangular spectrum is a reasonable approximation (*7*) and allows some useful conclusions to be drawn in the context of gradient shimming. Successful gradient shimming requires that the problem of fitting field maps with shim maps be significantly overdetermined. This sets a lower limit on the number n_s of significant data points which must be acquired across the signal profile. For a sample of length L in a uniform gradient G, the number of points acquired is

$$n_s = \frac{\gamma L G \tau_a}{2\pi}, \qquad [4]$$

where γ is the magnetogyric ratio of the nuclei concerned. This fixes an inverse relationship between G and τ_a; consequently one way to minimize the attenuation due to convection in Eq. [3] is to increase the read gradient G_r. Unfortunately this carries a proportionate and undesirable penalty in signal-to-noise ratio. Thus to use conventional gradient shimming methods in convecting samples requires sacrificing either, or both, digitization and sensitivity.

The additional phase shifts caused by a constant flow velocity can be refocused at τ_m by requiring (*7*, *8*) that the first moment of G^* also vanish:

$$\int_0^{\tau_m} G^*(t) t \, dt = 0. \qquad [5]$$

It is possible to satisfy conditions [1] and [5] simultaneously by adapting the sequence of Fig. 1a to form the symmetrical double spin–echo sequence shown in Fig. 1b. The symmetry about the central delay τ provides the required flow compensation; extra signal loss due to transverse relaxation is kept to a minimum by making the inner gradient pulses short and strong. The optional outer gradient pulses of width δ_1, shown with dotted lines in Fig. 1b, allow the sequence to be used with little or no phase cycling; the overall requirement for refocussing of Eq. [1] here reduces to

$$G_c \delta_2 = G_c \delta_1 + G_r \tau_a / 2. \qquad [6]$$

Figure 2 shows the effect of convection on profiles measured using the sequences of Figs. 1a and 1b for different solvents over a range of nominal probe temperatures. Experiments were carried out on a Varian Inova 400 MHz spectrometer equipped with a 5-mm PFG probe, with the variable temperature and cooling air flow rates both set to 10 L/min. After each temperature increment a stabilization delay of 20 min was allowed before the next experiment commenced. In general the vertical temperature gradient along a sample increases as the nominal sample temperature diverges from that under quiescent conditions. Convection currents are induced when a critical temperature gradient, determined by the solution viscosity and sample geometry, is reached. Despite careful probe design, temperature gradients, both vertical and horizontal, are unavoidable in practice. Indeed, in mobile solvents it is not uncommon to observe convection even at room temperature. The results of Fig. 2 show the effect of the increasing vertical sample temperature gradients as the nominal sample temperature is increased. As the gradients and hence the convection velocities increase, the distortion and attenuation of the profiles measured using sequence 1a become more apparent, to the point where the profiles are unusable. In contrast, the profiles measured with sequence 1b survive unscathed even when the samples approach their boiling points and convection is at its most rapid.

At the higher temperatures shown in Fig. 2, attempts to perform gradient shimming using the conventional sequence of Fig. 1a were unsuccessful. In contrast, good shim maps and rapid convergence were obtained using sequence 1b. Figure 3

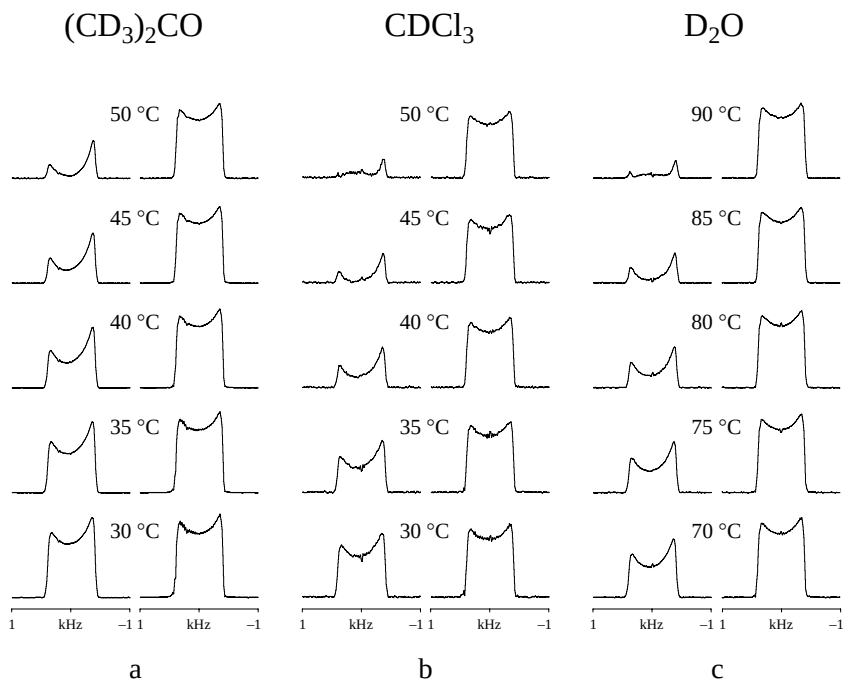

FIG. 2. Absolute value 61.4-MHz deuterium signal profiles as a function of nominal sample temperature measured with normal shimming using sequences 1a (left) and 1b (right) with $\tau_d = 10$ ms and $\tau_r = 2$ ms, respectively, for nonspinning samples of (a) acetone-d_6, (b) deuteriochloroform, and (c) deuterium oxide. Four transients of 64 complex points at a spectral width of 1 kHz (sequence 1a) or 128 complex data points at a spectral width of 2 kHz (sequence 1b) were acquired for each spectrum, corresponding to an acquisition time of 64 ms, with no delay τ and a recycle time of 30 s. The read gradient G_r for sequence 1b was approximately 0.8 G cm^{-1} and the spectral width was 2 kHz, with an inner gradient pulse width $\delta_2 = 2$ ms and an amplitude G_c of 10 G cm^{-1}; the optional pulses of width δ_1 were omitted.

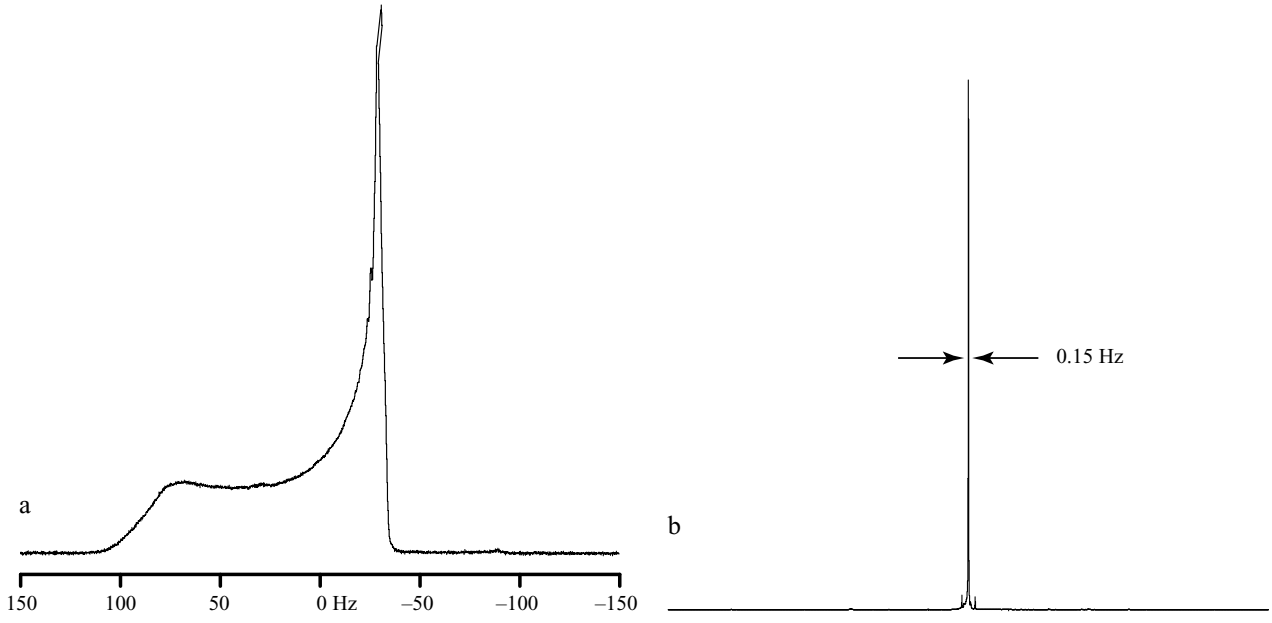

FIG. 3. (a) The 400-MHz nonspinning ^{1}H spectrum of TMS in deuterioacetone at 45°C, with all z shim currents set to zero; and (b) the spectrum recorded with sample spinning after less than 1 min of gradient shimming using the sequence of Fig. 1b.

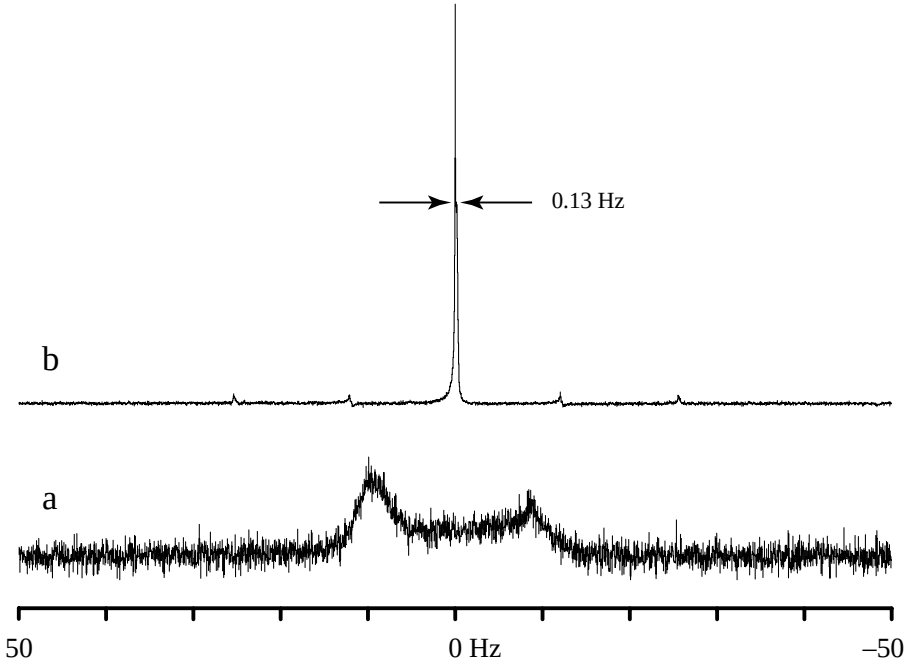

FIG. 4. (a) The 100-MHz nonspinning ^{13}C spectrum of TMS in deuterioacetone at 50°C, with poor transverse homogeneity and all *z* shim currents set to zero; and (b) the spectrum recorded with sample spinning after 5 min of gradient shimming using the sequence of Fig. 1c.

shows the change in ^{1}H lineshape obtained when the sequence of Fig. 1b was used to shim a sample of TMS in acetone-d_6 at a nominal temperature of 50°C, starting with all *z* shim currents set to zero. Excellent homogeneity was obtained within 1 min.

Not all probes allow the use of pulsed field gradients. In particular, probes for 10-mm samples very rarely offer such facilities, and gradient shimming has to rely on pulsing the *z* shim (homospoil pulsing). Here the slow response of the *z* gradient produced is a potential problem when designing suitable pulse sequences; it can take hundreds of milliseconds for the gradient produced by a homospoil pulse to decay below the background B_0 gradients. Figure 1c shows a modification of sequence 1b which is designed to use *z*-shim homospoil pulses. The relatively weak gradient strength allows the gradient to be left on during radiofrequency pulses, but the slow switch-on requires a small timing correction Δ, here 8 ms. Figure 4 shows the result of 5 min of *z* shimming using the sequence of Fig. 1d on a 10-mm acetone-d_6 sample at 50°C in a multinuclear probe, with poor transverse B_0 homogeneity and all *z* shims initially set to zero. The transverse inhomogeneity remains, as evidenced by the first and second order spinning sidebands in Fig. 4b, but the good linewidth of the spectrum shows correction of the *z* inhomogeneity to within the limits of the shim set used.

Gradient shimming has rapidly supplanted other methods for automated field correction, greatly reducing the time spent in manual shimming. Pulse sequences such as those of Fig. 1b and 1c, which are applicable to a range of nuclei and to a wide range of probes, extend the scope of gradient shimming to encompass the great majority of high-resolution NMR applications.

ACKNOWLEDGMENTS

This work was generously supported by the EPSRC (Grant GR/M16863), the Royal Society of Chemistry, and Pfizer Global Research and Development (RSC/EPSRC Analytical/CASE studentship to CLE).

REFERENCES

1. P. C. M. van Zijl, S. Sukumar, M. O'Neil-Johnson, P. Webb, and R. E. Hurd, *J. Magn. Reson. A* **111,** 203–207 (1994).
2. S. Sukumar, M. O'Neil-Johnson, R. E. Hurd, and P. C. M. van Zijl, *J. Magn. Reson.* **125,** 159–162 (1997).
3. H. Barjat, P. B. Chilvers, B. K. Fetler, T. J. Horne, and G. A. Morris, *J. Magn. Reson.* **125,** 197–201 (1997).
4. P. B. Chilvers and G. A. Morris, *J. Magn. Reson.* **133,** 210–215 (1998).
5. H. C. Torrey, *Phys. Rev.* **104,** 563–565 (1956).
6. P. T. Callaghan, "Principles of Nuclear Magnetic Resonance Microscopy," Oxford Univ. Press, Oxford (1991).
7. N. M. Loening and J. Keeler, *J. Magn. Reson.* **139,** 334–341 (1999).
8. A. Jerschow and N. Müller, *J. Magn. Reson.* **125,** 372–375 (1997).